Eur. Phys. J. E (2019) **42**: 100
DOI 10.1140/epje/i2019-11862-3

THE EUROPEAN PHYSICAL JOURNAL E

Regular Article

The cooperative free volume rate model for segmental dynamics: Application to glass-forming liquids and connections with the density scaling approach*

Ronald P. White and Jane E.G. Lipson[a]

Department of Chemistry, Dartmouth College, Hanover, NH 03755, USA

Received 29 May 2019 and Received in final form 26 June 2019
Published online: 12 August 2019

Abstract. In this paper, we apply the cooperative free volume (CFV) rate model for pressure-dependent dynamics of glass-forming liquids and polymer melts. We analyze segmental relaxation times, τ, as a function of temperature (T) and free volume ($V_{\rm free}$), and make substantive comparisons with the density scaling approach. $V_{\rm free}$, the difference between the total volume (V) and the volume at close-packing, is predicted independently of the dynamics for any temperature and pressure using the locally correlated lattice (LCL) equation-of-state (EOS) analysis of characteristic thermodynamic data. We discuss the underlying physical motivation in the CFV and density scaling models, and show that their key, respective, material parameters are connected, where the CFV b parameter and the density scaling γ parameter each characterize the relative sensitivity of dynamics to changes in T, *vs.* changes in V. We find $\gamma \approx 1/[b(V_{\rm free}/V)_{@T_{\rm g}}]$, where $(V_{\rm free}/V)_{@T_{\rm g}}$ is the value predicted by the LCL EOS at the ambient $T_{\rm g}$. In comparing the predictive power of the two models we highlight the CFV advantage in yielding a universal linear collapse of relaxation data using a minimal set of parameters, compared to the same parameter space yielding a changing functional form in the density scaling approach. Further, we demonstrate that in the low data limit, where there is not enough data to characterize the density scaling model, the CFV model may still be successfully applied, and we even use it to predict the correct γ parameter.

1 Introduction

In this article, we focus on modeling α-relaxation times (τ) obtained via broadband dielectric spectroscopy (BDS) using the cooperative free volume (CFV) rate model [1–3]. In addition, we draw comparisons with the "density scaling approach" [4–12], another model well known for application to BDS data. CFV and density scaling each offer physical explanations for interpreting and understanding dynamics, and in this work we compare and discuss their underlying physical frameworks, relate their key parameters, and show how they are connected.

CFV and density scaling are models for "pressure-dependent dynamics" [4,5], meaning that they describe $\tau(T,V)$, and thus account for the independent contributions from both temperature (T) and volume (V). This allows a more detailed understanding of the underlying physics than could be obtained by only characterizing the T-dependence under ambient pressure, where T and V are both changing. In the density scaling approach, dynamics are a function of the combined variable, TV^{γ}, where γ is a material specific parameter. An explanation for this form (see sect. 2) is that the dynamics are being dictated by each system's characteristic short-ranged intermolecular repulsions. In CFV, intermolecular repulsions are also important but they are addressed in a different way.

The CFV model approaches dynamics in terms of an activated, volume-dependent, rate mechanism. Short-range repulsions that are "thermally accessible" must be overcome by thermal activation. Otherwise these repulsions contribute to the system's limiting closely packed hard-core volume which, when subtracted from the total volume, allows quantification of the remaining "free space" ($V_{\rm free}$). The available free volume determines the local need for cooperativity (*i.e.*, how many segments must be involved), which directly determines the total activation energy required for segments to rearrange.

Here it is critical to note explicitly that, while the CFV model quantifies free volume and illustrates its role as a natural variable in analyzing dynamics data, it also

* Contribution to the Topical Issue "Dielectric Spectroscopy Applied to Soft Matter" edited by Simone Napolitano.

[a] e-mail: jane.lipson@dartmouth.edu
(corresponding author)

leads to a functional form that has explicit T-dependence. The latter is essential in order to understand dynamic relaxation. In contrast, historical free volume models based on the Doolittle equation [13–16], assume that dynamics depends on free volume *alone*. This assumption is clearly wrong (at least for any meaningful definition of free volume), as shown by P-dependent dynamics experiments and comparisons with corresponding volumetric data [4, 5,17,18]. In addition to applying the CFV model to the P-dependent dynamics of bulk material, we have recently used it to predict the temperature and thickness dependence of dynamic relaxation in polymer thin films [1,19], which highlights the importance of accounting for density changes in the dynamics of confinement.

In the remainder of this paper, background on the density scaling approach will be covered in sect. 2, and in sect. 3 we turn to the CFV model. Modeling results for a variety of polymer and small molecule glass-forming liquids will be presented in sect. 4, where we will also discuss connections between the CFV and density scaling approaches, including comparisons of their predictive power. A summary is given in sect. 5.

2 The density scaling approach

In its most basic interpretation, the density scaling approach can be described as the expectation that general P-dependent dynamics data can be expressed (collapsed) such that relaxation times are given by $\tau = F(TV^\gamma)$, where τ is a function of the single combined variable, TV^γ, where γ is a material specific parameter, and where F is some function of unspecified form. Examples of collapsed plots of τ *vs.* TV^γ are common in the literature, *e.g.*, see figs. 16 and 17 in the review by Roland *et al.* [4], and one illustrative example is also given here for polyvinyl acetate (PVAc) showing $\log\tau$ *vs.* $1/(TV^\gamma)$ in fig. 1 further below. Clearly this expectation about the scaling behavior of the dynamics is satisfied by a very large number of systems, so it is important to have physical explanations that address this behavior at the molecular level.

The power law form of density scaling can be appreciated by considering the simple, purely repulsive, inverse power law (IPL) fluid. An IPL has a pair potential, $u(r) \propto 1/r^n$, leading to a simple form for the excess partition function, which depends (in scaled coordinates) only on the single variable $TV^{n/3}$. This leads to dynamic properties that are also a function of $TV^{n/3}$ [20,21], where we now identify $n/3 = \gamma$.

The "isomorph theory" of Dyre and coworkers [8,9] has done much to explain why many real systems, which are of course not simple IPL's, can also satisfy density scaling. When a real system satisfies density scaling, it is a consequence of that system having strong pressure-energy correlations. Importantly, the IPL fluid has exact pressure-energy correlations, where, instantaneous fluctuations in the virial, ΔW, and in the corresponding potential energy, ΔU, relate exactly as $\Delta W = (n/3)\Delta U = \gamma\Delta U$. In more realistic systems, the instantaneous pressure-energy correlations are not exact, but, they are often still "strong", and thus, $\Delta W \approx \gamma\Delta U$, and this is a metric defining the "simple Roskilde system" [8].

The framework offers ways to understand *dynamics*, by making connections with the underlying *thermodynamic* properties. The simulation works of Pedersen *et al.* [22, 23] and Coslovich and Roland [24–26] have shown that the averaged pressure-energy correlations for Lennard-Jones–type systems can be mapped to a corresponding, simpler, IPL fluid, specifically, the one that has the same pressure-energy correlations. Here γ is thus identified as the average (statistical) slope of W *vs.* U, *i.e.* $\gamma \approx \langle \Delta W \Delta U\rangle / \langle (\Delta U)^2 \rangle$, which is based on *thermodynamics*, and this γ value successfully collapses the (T,V)-dependent *dynamics* data.

In addition to this background relating the approach to simulated model fluids, density scaling with the γ parameter has been widely applied in the analysis of P-dependent dynamics data for real experimental systems (*e.g.*, studied by BDS). Here, due to the lack of detailed thermodynamic information of the sort described above, the value for γ must typically be determined by fitting experimental dynamics data. Real experimental systems have commonly been modeled using the analytic $\tau(T,V)$ expression developed in Casalini *et al.* [11,12] where the T, V density scaling form was derived using the Avramov entropy model [27], and this is given by

$$\ln\tau = \left(\frac{A}{TV^\gamma}\right)^\phi + \ln\tau_0 \tag{1}$$

Equation (1) includes the γ parameter, along with three other material specific parameters, ϕ, A, and τ_0. In Casalini and Roland [12] there are examples showing (linearized) $\log\tau$ *vs.* $(1/TV^\gamma)^\phi$ plots, along with tabulations of the fitted parameters for a number of polymer and small molecule systems.

Finally, we note that in density scaling the dynamics properties should be written/analyzed in reduced variables [8–10,20,21,24]. For simplicity, this analytic correction can often be neglected, as it is here in analyzing the experimental BDS results, because in this regime the strong activation energies will dominate. However, using reduced variables does become important in the high T regime, otherwise the data will not collapse. In fact, the reduced variable analysis in density scaling is related to the way in which the CFV rate model treats its pre-exponential factor in order to capture properly the effects of temperature in that regime.

3 The cooperative free volume rate model

As in density scaling, the CFV rate model [1–3] describes segmental relaxation times as a function of temperature and volume, $\tau(T,V)$. A key ingredient in CFV is the system's thermodynamically characterized free volume. $V_{\rm free}$ is defined as the difference between a system's overall volume, V, and its limiting, closely packed, hard-core value, $V_{\rm hc}$:

$$V_{\rm free} = V - V_{\rm hc}; \tag{2}$$

$V_{\rm hc}$ is a constant for each system, independent of both T and P, and quantifies the system's minimum possible volume. It arises from the strong intermolecular repulsions (the lingering molecular hard cores) that cannot be "reasonably overcome" by thermal activation, and is determined via analysis of experimental PVT data using the locally correlated lattice (LCL) model equation of state (EOS) [17,28]; some details related to this are provided in the appendix.

The physical basis of the CFV rate model involves a cooperative process in which the total activation free energy for segmental relaxation, $\Delta A_{\rm act}$, changes with the number, n^*, of cooperating particles (segments); an analogy can be drawn to the well-known treatment of Adam and Gibbs [29], a model based on entropic considerations.

In CFV the system is characterized by an average free volume per particle, $V_{\rm free}/N$. For a segment to break out of the cage of its surrounding neighbors and move, a characteristic amount of free space (v^*) is needed. The total number of nearby segments required to cooperate and open up this space is $n^* = v^*/(V_{\rm free}/N)$. Each cooperating segment pays an energetic cost, Δa, associated with overcoming thermally accessible repulsions, as well as attractions. This adds up to give the overall total activation energy, $\Delta A_{\rm act} = n^* \Delta a$. The CFV machinery explains the volume dependence of the activation energy, and why systems follow a $1/V_{\rm free}$ form in their volume dependence.

The rate ($\propto 1/\tau$) that a segment enters a new opening is proportional to the rate it traverses a distance on the order of its own size ($\propto$ velocity $\propto T^{1/2}$), multiplied by the probability that a free space is available, given by the Boltzmann factor, $\exp[-\Delta A_{\rm act}/T]$. The general result is

$$1/\tau = \text{rate} = [\text{constant}] \times T^{1/2} \times \exp\left[-n^* \times \left(\frac{\Delta a(T)}{T}\right)\right]$$
$$= [\text{constant}] \times T^{1/2} \times \exp\left[-\left(\frac{1}{V_{\rm free}}\right) \times f(T)\right]. \quad (3)$$

The activation free energy per cooperating segment, $\Delta a(T)$, is some unknown function of temperature, but not of volume. In fact, in our simulation results, which cover a very wide range of the high T regime, a constant value of Δa is sufficient in eq. (3). Given an *a priori* PVT analysis for $V_{\rm hc}$, one can then express all the system's high T regime $\tau(T,V)$ dynamics behavior, including non-Arrhenius behavior, with just two constant parameters, Δa and the limiting τ. The fact that constant Δa works at high T provides an especially clear demonstration of how the total $\Delta A_{\rm act}$ depends on volume.

A key point to highlight is the importance of the gas kinetic $T^{1/2}$ in the high-T regime, *e.g.* a regime commonly accessed in simulation studies. As noted above, in density scaling, using a reduced τ appropriately brings in the $T^{1/2}$ term. However, outside of the simulation works in the density scaling community, the gas kinetic correction has often been neglected in the analysis of simulation data [2,3], and the result may be activation energies that are incorrect. These details are not a problem at lower T in glassy systems, where activation energies become high enough that the gas kinetic term can be dropped for simplicity.

For the latter scenario, eq. (3) leads to the following working form of the CFV equation, which is applicable for BDS studies on experimental liquids:

$$\ln \tau = \left(\frac{V_{\rm hc}}{V_{\rm free}}\right)\left(\frac{T^*}{T}\right)^b + \ln \tau_{\rm ref}, \quad (4)$$

where b, T^*, $\tau_{\rm ref}$, are material specific parameters. Here we use the relative free volume, $V_{\rm free}/V_{\rm hc}$, (*e.g.*, rather than $V_{\rm free}/N$) because it is convenient. The form of the T-dependence, $\Delta a(T)/T = f(T) \sim 1/T^b$, is empirical, but it has been found to work very well. We apply eq. (4) to a variety of experimental systems below. It turns out that there is a strong connection between the b parameter and the γ parameter. Indeed, they are analytically related, as discussed further below.

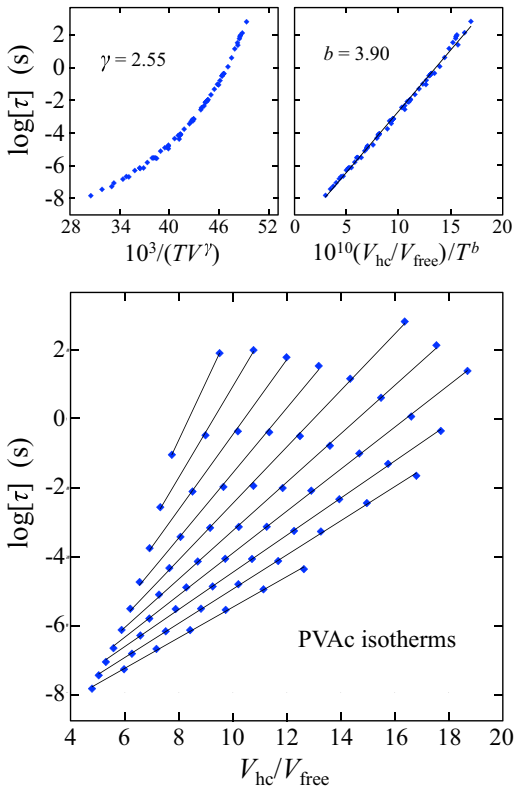

Fig. 1. (T,P)-dependent α-relaxation times (τ) for PVAc. Main panel: $\log \tau$ *vs.* inverse relative free volume ($V_{\rm hc}/V_{\rm free}$), plotted as isotherms. Symbols mark each experimental relaxation time at the corresponding $V_{\rm hc}/V_{\rm free}$ value, calculated independently via LCL EOS analysis of the PVT data. References for experimental data are available in table 1. Isotherms range from $T = 323$ to 413 K in increments of 10 K (lines are the corresponding linear fits); pressure values range from 1 atm up to as high as 400 MPa. Upper panels: collapsed plots of the same (T,P)-dependent data. Density scaling, upper left: $\log \tau$ *vs.* $1/TV^\gamma$ where $\gamma = 2.55$ (T in K, V in mL/g). CFV model, upper right: $\log \tau$ *vs.* $(V_{\rm hc}/V_{\rm free})/T^b$ where $b = 3.90$ (T in K).

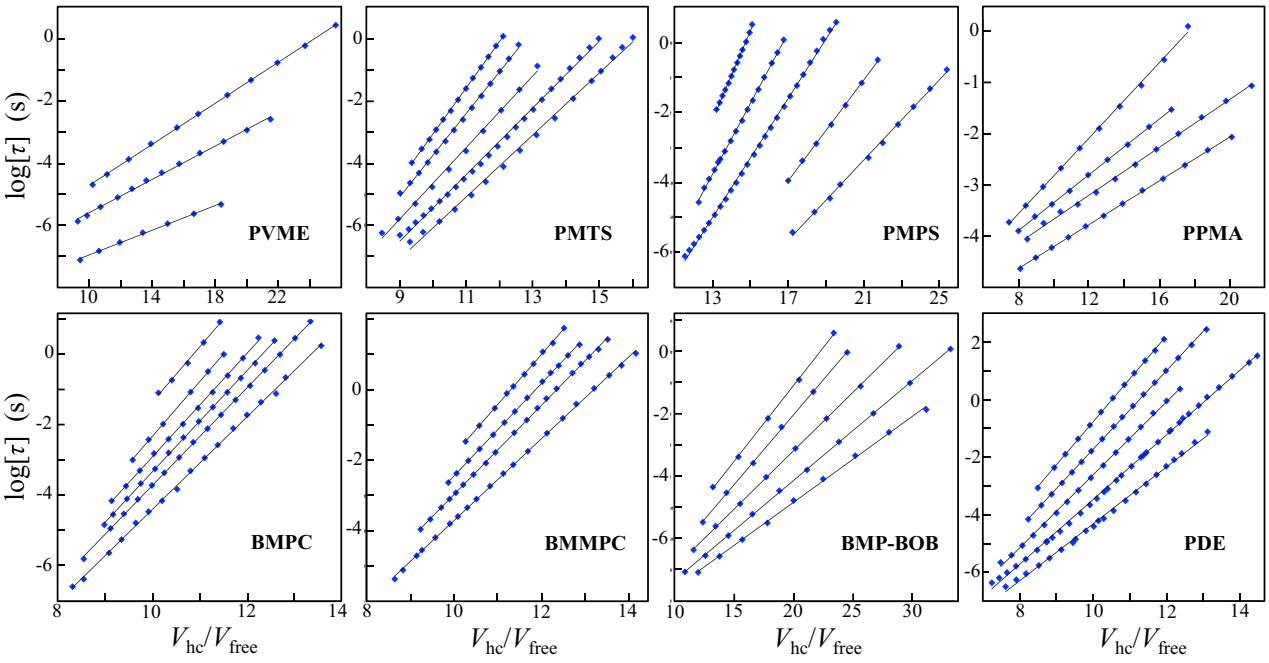

Fig. 2. (T, P)-dependent α-relaxation times (τ) plotted as $\log\tau$ *vs.* $V_{\rm hc}/V_{\rm free}$ isotherms, for polymer and small molecule liquids: PVME, PMTS, PMPS, PPMA, BMPC, BMMPC, BMP-BOB, and PDE. Acronyms and references for experimental data are available in table 1. Symbols mark each experimental relaxation time at the corresponding $V_{\rm hc}/V_{\rm free}$ value, the latter calculated independently via LCL EOS analysis of the PVT data, and lines are the corresponding linear fits.

4 Results and discussion

The CFV rate model eq. (3) *predicts* that $\log\tau$ *vs.* $1/V_{\rm free}$ will exhibit a linear relationship on isotherms, and that the isotherm slopes ($\propto \Delta a(T)/T$) will increase with decreasing T. Figures 1 and 2 clearly demonstrate that this is indeed the case for a variety of experimental systems ranging from small molecule glass-forming liquids to polymer melts (references in table 1). Here the experimental relaxation times ($\log\tau$) have been plotted as isotherms against the corresponding inverse relative free volume values ($V_{\rm hc}/V_{\rm free}$) that were determined, independently, from an *a priori* analysis of each system's PVT data using the LCL EOS. For all these systems the isotherms are linear, and the slopes increase with decreasing T.

Results using this analysis also serve to emphasize that a single $V_{\rm free}$ value will *not* correspond to a single τ value, and that accounting for temperature is essential. In contrast, the Doolittle equation [13] assumes that dynamics are a function of free volume alone.

The general $\log\tau \sim (1/V_{\rm free}) \times \Delta a(T)/T$ form of the CFV model appropriately predicts that the lower the temperature, the more strongly the system will react to (free) volume changes, and similarly, the lower the volume, the more strongly the system will react to temperature changes. This T-V coupling in real system dynamics is thus explained by CFV as being a mechanistic consequence of density-based cooperativity, where changing inverse free volume acts multiplicatively, to scale up the activation energy inside the Boltzmann factor (eq. (3)). We have recently used these arguments to explain why, in confined systems, the sensitivity to confinement increases upon lowering of T [19], as changing degree of confinement relates to changing average density.

Next we show the application of CFV eq. (4). The correct, material-dependent, value of b will collapse all T, V data in a plot of $\log\tau$ *vs.* $1/(T^bV_{\rm free})$; in a sense this is analogous to how the correct density-scaling γ value will collapse a plot of $\log\tau$ *vs.* $1/TV^\gamma$. However, while $\log\tau$ *vs.* $1/TV^\gamma$ collapses data into a *single curve*, $\log\tau$ *vs.* $1/(T^bV_{\rm free})$ yields a *single line*. The upper panels of fig. 1 demonstrate this comparison for PVAc.

The collapsed curve for the case of density scaling corresponds to $\gamma = 2.55$. For CFV, a linear collapse is obtained where $b = 3.90$. (Here both γ and b were determined by simple trial and error adjustment.) Because the CFV collapse forms a single line, the remaining parameters, T^* and $\tau_{\rm ref}$, then follow immediately from the slope ($0.4343\ T^{*b}$) and intercept ($\log\tau_{\rm ref}$) of the $\log\tau$ *vs.* $V_{\rm hc}/(T^bV_{\rm free})$ plot, and this completely characterizes the model for the given system. Figure 3 shows the collapsed linear plots of $\log\tau$ *vs.* $(V_{\rm hc}/V_{\rm free})(T^*/T)^b$ for each system, along with the corresponding system-specific b value.

Table 1 summarizes the system CFV and LCL EOS parameters, along with the corresponding γ parameters from density scaling, and system information and references to the experimental dynamics and PVT data.

Next, we compare the key material specific parameters from density scaling and CFV. As described in sects. 2 and 3, γ is the key parameter for density scaling, and b is key in CFV. Some important identities for each are covered in the following.

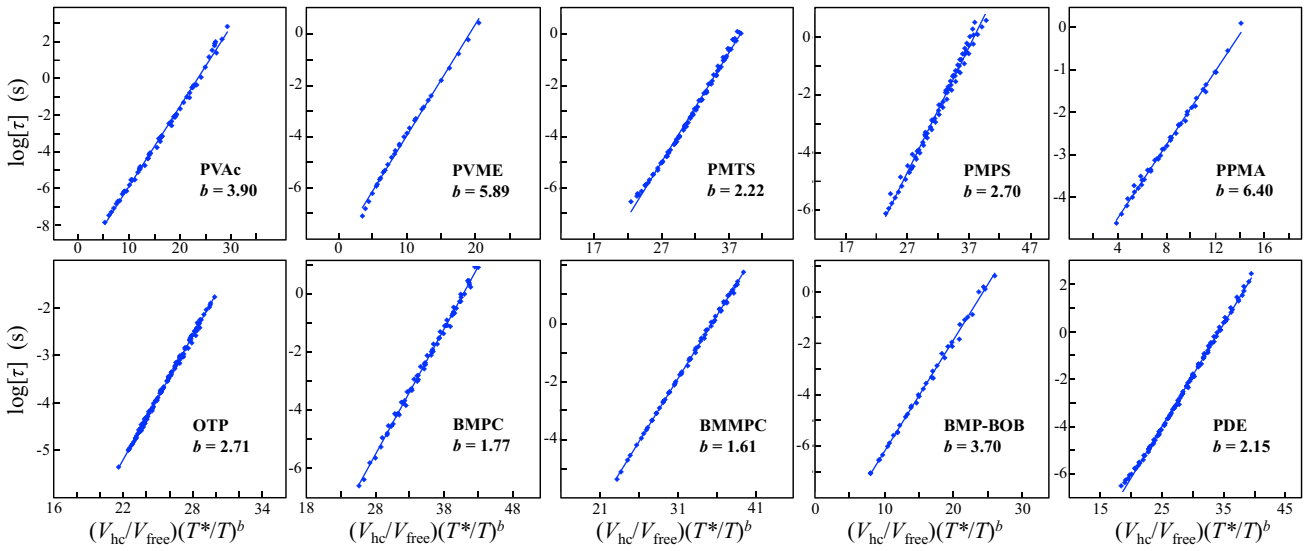

Fig. 3. (T, P)-dependent relaxation times plotted according to CFV eq. (4), $\log\tau$ *vs.* $(V_{\rm hc}/V_{\rm free})(T^*/T)^b$, where each system's material specific b value collapses the data, leading to full model characterization. (Lines demonstrate the model fit.) Systems include polymer and small molecule liquids: PVAc, PVME, PMTS, PMPS, PPMA, OTP, BMPC, BMMPC, BMP-BOB, and PDE. Acronyms and references for experimental data are available in table 1. Note OTP did not appear in fig. 2 because the P-dependent data was not given in the form of isotherms, though the resulting collapsed data is demonstrated here.

In density scaling, given that τ is a function of the single combined variable, TV^γ, one can write for any two states that have the same τ value (isochronic states), $(T_2/T_1) = (V_1/V_2)^\gamma$, and, when T_1, T_2, V_1, V_2 are known, then it is possible to solve for the system's γ value. It is relevant to note that this can also provide a possible route for obtaining γ when actual dynamics data are not available, for example, when the glass transition temperatures, $T_{\rm g}$, are known at two different pressures from PVT data (assuming these to be isochronic points). This isochronic relationship can be equivalently written for γ as

$$\gamma = -\left(\frac{\partial \ln T}{\partial \ln V}\right)_\tau . \tag{5}$$

Analogously, in CFV, inspection of eq. (4) shows that τ is expected to be a function of the single combined variable, $T^b V_{\rm free}$, and one can write $(T_2/T_1)^b = (V_{\rm free,1}/V_{\rm free,2})$ for any two isochronic points. Just as for γ, this yields a solution for b from PVT-based $T_{\rm g}$ values (*e.g.*, for P4ClS in ref. [1]); the analogous derivative relationship for b is given by

$$b = -\left(\frac{\partial \ln V_{\rm free}}{\partial \ln T}\right)_\tau . \tag{6}$$

Equations (5) and (6) illustrate that γ and b both serve as a metric, characterizing a system's relative sensitivity to changes in temperature compared to changes in volume. These metrics are important in P-dependent dynamics investigations for comparing different material systems. Another commonly used characteristic quantity is the value of E_V/E_P, the ratio of activation energies, $\mathrm{d}\ln\tau/\mathrm{d}(1/T)$, at constant V, and at constant P. Equation (5) shows that a high γ value indicates a strong sensitivity to volume, *i.e.* upon a change in $\ln V$, a relatively large change in $\ln T$ would be required to balance it out to keep τ the same. According to eq. (6), a strong sensitivity to volume, based in terms of "free volume", would correspond to a low value of b.

Given the above, it is sensible to expect that when we compare systems modeled by both density scaling and CFV, that there should be a correlation where systems with high γ will have low b values, and visa-versa, and indeed this is true. This comparison, for 11 small molecule and polymer systems, is presented in the upper panel of fig. 4. The γ values are from independent analyses and no connection to CFV has been assumed; most values were taken directly from the literature. There is some scatter in the correlation, but as expected, an approximate inverse relationship between γ and b is fairly apparent.

In fact, an exact relationship between γ and b can be derived. The expression for γ (eq. (5)) can be rewritten in terms of a change in $\ln V_{\rm free}$ and this gives

$$\begin{aligned}\gamma &= -\left(\frac{\partial \ln T}{\partial \ln V}\right)_\tau = -\left(\frac{\partial \ln T}{\partial \ln V_{\rm free}}\right)_\tau \frac{\mathrm{d}\ln V_{\rm free}}{\mathrm{d}\ln V} \\ &= -\left(\frac{\partial \ln T}{\partial \ln V_{\rm free}}\right)_\tau \frac{V}{V_{\rm free}} .\end{aligned} \tag{7}$$

In eq. (7), $\mathrm{d}\ln V_{\rm free}/\mathrm{d}\ln V = V/V_{\rm free}$ follows from the simple definition, $V_{\rm free} = V - V_{\rm hc}$ (eq. (2)), where $\mathrm{d}V_{\rm free}/\mathrm{d}V = 1$. Substituting eq. (6) into eq. (7) we obtain the relationship between γ and b:

$$\gamma = \frac{1}{b(V_{\rm free}/V)} \approx \frac{1}{b(V_{\rm free}/V)_{@T_{\rm g}}} . \tag{8}$$

Equation (8) shows that the relationship between γ and b technically carries a density dependence due to the

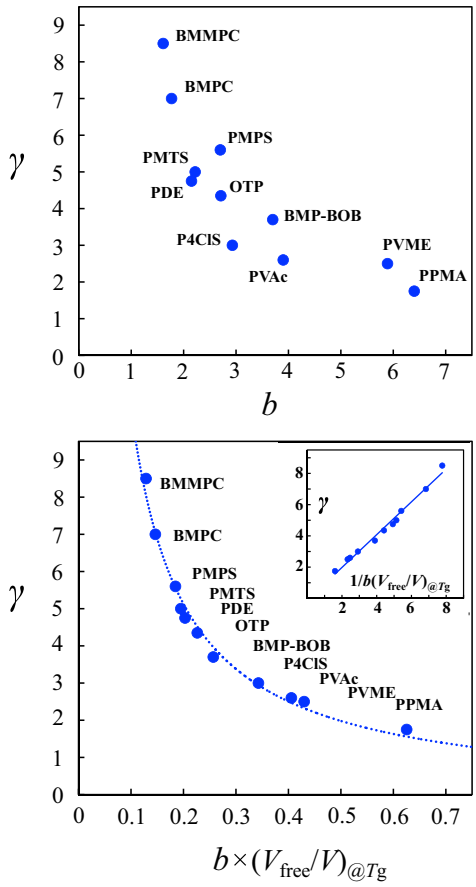

Fig. 4. Relationship between the γ parameter and the CFV b parameter for polymers and small molecule liquids. Upper panel: scatter plot of system γ values *vs.* system b values. Lower panel: γ *vs.* $b(V_{\rm free}/V)_{@T_{\rm g}}$ (with smooth fit hyperbola). Lower panel inset: γ *vs.* $1/(b(V_{\rm free}/V)_{@T_{\rm g}})$ (with corresponding linear fit). System acronyms are marked in the figure. Acronyms definitions and references for γ values and experimental data are available in table 1.

presence of the multiplicative factor, $V_{\rm free}/V$, the fractional free volume. However, we can still accurately convert between the two parameters. Over the "operating range" of the P-dependent analysis, $V_{\rm free}/V$ may vary by about a factor of two, so in what follows we choose a single $V_{\rm free}/V$ value that is representative of the average $V_{\rm free}/V$ of this range. It is sensible to expect that this should work because we know that a constant b and a constant γ each work well describing data within their respective model frameworks. The $V_{\rm free}/V$ value at the *ambient* $T_{\rm g}$ is a good single choice. This is because, being at a low T, but also, low P, gives it an intermediate density, putting it roughly in the middle of the range of the $V_{\rm free}/V$ values over a typical P-dependent data set.

We denote the $V_{\rm free}/V$ value at the system ambient $T_{\rm g}$ as $(V_{\rm free}/V)_{@T_{\rm g}}$, and this gives the operating relationship connecting each system's γ and b, $\gamma \approx 1/[b(V_{\rm free}/V)_{@T_{\rm g}}]$, which is the right-hand form in eq. (8). The lower panel of fig. 4 shows this is a very accurate description; all systems fall neatly onto the γ *vs.* $b(V_{\rm free}/V)_{@T_{\rm g}}$ hyperbola. (A corresponding linearized plot of γ *vs.* $1/[b(V_{\rm free}/V)_{@T_{\rm g}}]$ is shown in the inset.)

Being able to obtain b from a density scaling analysis, or, γ from a CFV analysis, is a powerful new connection, leading to more insight, and allowing conversion between literature results. For example, Casalini and Roland [30] presented and tested an approximate relationship for obtaining the γ parameter from ambient data only, $\gamma = V\Delta\alpha_P/(\Delta c_P\kappa_T - TV\alpha_P\Delta\alpha_P)$. This requires knowing the liquid's coefficients of thermal expansion (α_P) and compressibility (κ_T), and some information on the glass, including the differences (liquid relative to glass) in heat capacity (Δc_P), and in coefficient of thermal expansion ($\Delta\alpha_P$). The relationship assumes that, at $T_{\rm g}$, τ is a constant, *i.e.* the glass transition point is defined as a kinetic event, and, that the Erhenfest equation for entropy continuity holds at this point. Though the latter is an expectation that cannot be guaranteed, tests in ref. [30] do show good performance in predicting γ for a number of systems. (The Erhenfest equation based on entropy continuity has been verified to hold for many systems (though not always), while the equation based on volume continuity often does not hold [30–32].) Given the new relationship provided by eq. (8), this route can now be applied to obtain the CFV b parameter as well, *i.e.* $b \approx (\Delta c_P\kappa_T - TV\alpha_P\Delta\alpha_P)/(V\Delta\alpha_P(V_{\rm free}/V)_{@T_{\rm g}})$.

Next we compare the density scaling and CFV models in terms of predictive power, an indication of how well a model anticipates the behaviour reflecting the underlying physics. In order to fit the dynamics data, the density scaling equation (eq. (1)) requires the specification of four parameters $(\gamma, \phi, A, \tau_0)$. By comparison the CFV equation (eq. (4)) only requires the specification of three parameters $(b, T^*, \tau_{\rm ref})$. This is because CFV brings *thermodynamic* information through the prediction of $V_{\rm hc}$ (thus all $V_{\rm free}$ values) via the *a priori* analysis of PVT data. (Note PVT data are required by both models, being needed to express $V(T,P)$, which means that the separate thermodynamic characterization for $V_{\rm hc}$ and $V_{\rm free}$ represents no added data burden.)

In density scaling one starts the parameterization not knowing the form of either the volume or temperature dependence, since values for the scaling exponents γ and ϕ are unknown. In CFV, we start by not knowing the T-dependence (b), *however*, the form of the volume contribution has been specified: all systems follow the $1/V_{\rm free}$ form. $V_{\rm free}$ can be determined without information on dynamics, and this is a key advantage of the approach.

To demonstrate, we show the application of the CFV model in two cases where the application of density scaling is not possible. These examples, shown in fig. 5, make use of the pressure-dependent dynamics data for PVAc, plotted as $\log\tau$ *vs.* $1/T$ isobars. Density scaling requires four data points in order to fit its four parameters, and here, fewer than four points are allowed for model fitting. While a difference in the availability of just one data point may not be important in many scenarios, when comparing models in the hypothetical low data limit,

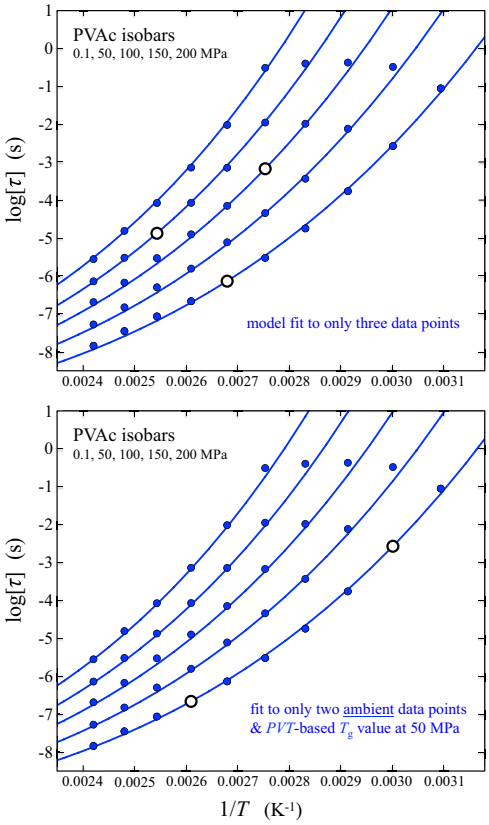

Fig. 5. (T, P)-dependent α-relaxation times (τ) for PVAc, plotted in the form of $\log\tau$ *vs.* $1/T$ isobars. Plots show the results of fitting the CFV model to only the data at the marked points (large hollow symbols); the model curves are predictions to be compared with the remaining experimental data (smaller blue points). Using only the marked data points, alone, density scaling cannot be applied. Upper panel: CFV model fit to only three data points, giving fitted b, T^*, $\log\tau_{\rm ref}$ values of 3.58, 427 K, −10.3, respectively. Lower panel: CFV model fit to only two data points that are both restricted to ambient pressure, along with a PVT-based $T_{\rm g}$ value at $P > 1$ atm (here, 50 MPa), giving fitted b, T^*, $\log\tau_{\rm ref}$ values of 3.67, 421 K, −10.1, respectively. Experimental references are available in table 1.

a difference of one data point is indeed very significant from a *physical* standpoint.

The upper panel of fig. 5 shows the result of fitting the CFV model ($b, T^*, \tau_{\rm ref}$ in eq. (4)) to just three dynamics data points (marked by the large hollow symbols); the resulting model *predictions* are shown as the set of blue curves. The CFV predictions (curves) are in excellent agreement with the remaining P-dependent data (smaller blue points), which were unknown to the model before the fit. As noted above, density scaling cannot be applied here, and furthermore, it is not possible to determine even just the γ parameter alone; this is because, even though the three data points give information at varied pressure values, none of the points are isochronal, so one cannot apply the eq. (5) relationship. Furthermore, it is also impossible to uniquely identify γ by "collapsing" the data, because, with three points, any γ value would give a connecting "curve". By contrast, in CFV, b is chosen so that the three points collapse and form a unique straight line.

Though there is not enough information to apply density scaling to obtain γ, the CFV model can in fact deliver the γ value. The small amount of data was enough to determine b (as well as T^* and $\tau_{\rm ref}$), and so γ can be obtained from $\gamma \approx 1/[b \times (V_{\rm free}/V)_{@T_{\rm g}}]$. Specifically, the 3-point fit in fig. 5 gives $b = 3.583$, and the $(V_{\rm free}/V)_{@T_{\rm g}}$ value calculated via the LCL EOS is 0.104. This gives (using eq. (8)) a CFV prediction of $\gamma = 2.68$, which is in excellent agreement with the PVAc γ value of 2.6 from Roland *et al.* [4, 33] and 2.55 shown in the data collapse of fig. 1.

The lower panel of fig. 5 shows another situation in which the data are sparse. In this case the CFV model is characterized by fitting only two $\{\tau, T\}$ BDS dynamics data points at ambient pressure (which means there is no information on data curvature), and the only pressure-related information given for fitting is from PVT data, where we used the PVT-based ambient $T_{\rm g}$, coupled with a single $T_{\rm g}$ value at elevated pressure. All the remaining curves in fig. 5 are the CFV predictions for $P > 1$ atm, and the agreement with experimental data (blue symbols) is clearly excellent.

In this latter example, we utilized the PVT-based $T_{\rm g}$ information at elevated pressure to first obtain the CFV b parameter, and this same information can also be used to obtain the γ parameter. As described above, *a priori* estimates for both γ and b can be obtained from the isochronic relationships of $(T_2/T_1) = (V_1/V_2)^\gamma$ and $(T_2/T_1)^b = (V_{\rm free,1}/V_{\rm free,2})$, respectively. Inputting the T, V values and T, $V_{\rm free}$ values for the PVAc $T_{\rm g}$ point "1" at ambient P, and its $T_{\rm g}$ point "2" at $P = 50$ MPa (details in ref. [1]), we obtain an estimate of $\gamma = 2.87$ and $b = 3.67$.

The CFV parameterization of eq. (4) in the lower panel of fig. 5 was successful because, with the b value known, only two parameters remain (T^* and $\tau_{\rm ref}$), and so the two given ambient pressure dynamics data points are sufficient to fit them, thereby fully characterizing the model and allowing the predictions to be generated. This is not the case for density scaling because, even though we were able to obtain the γ value, three parameters in eq. (1) still remain unspecified and the two data points available for fitting are not enough to fully parameterize the model. (Perhaps somewhat ironically, the VFT equation, just for the ambient dynamics, also cannot be fit with only those two ambient points.)

Application of the CFV model is thus possible in cases where limitations of data preclude using density scaling. However, even the CFV approach is stymied if only ambient data are available - both relaxation times and glass transition temperature. A 3-parameter CFV fit of b, (along with T^*, and $\tau_{\rm ref}$) to ambient dynamics data, alone, is likely to fit the curvature reflecting ambient response too closely. On the other hand, there is still some information that can be extracted using the basic eq. (3) framework of CFV, *e.g.* to make some rough approximate predictions (*e.g.*, set bounds) for a system's pressure-dependent dynamics. We will address this topic in future work.

Table 1. System dynamics parameters (b, T^*, and $\tau_{\rm ref}$ are system-dependent parameters for the CFV model; most were obtained by simultaneous 3-parameter fitting of the $\tau(T,P)$ data to eq. (4); as noted, first collapsing data for b, followed by a linear fit for T^* and $\tau_{\rm ref}$ gives similar results. γ is a system-dependent parameter for the density scaling approach. Most of the γ values come from table 2 of Roland *et al.* review [4]. For the remaining values: γ for BMB-BOB is from ref. [34]; γ for PPMA was obtained in this work by collapsing the $\log\tau$ *vs.* $1/TV^\gamma$ data, and also for OTP (because $\gamma = 4.35$ gives a somewhat better collapse of the dielectric data [35] than the commonly reported $\gamma = 4.00$); the γ for P4ClS is via PVT-based $T_{\rm g}(P)$ [1,36] and eq. (38) of ref. [4]), EOS parameters (the LCL equation-of-state molecular parameters are: r, the number of segments (occupied lattice sites) per molecule, v, the volume per lattice site, and ε, the segment-segment nonbonded interaction energy. $M_{\rm w}$ is molecular weight. The hard-core volume, $V_{\rm hc}$, per molecule, is obtained from the product, rv, and $V_{\rm free}$ is thus defined as $V - V_{\rm hc}$. See the appendix for more information on LCL EOS implementation) and experimental references. System acronyms and info: PVAc: polyvinylacetate, PVME: polyvinylmethylether, PMPS: poly methylphenylsiloxane, PMTS: poly methyltolylsiloxane, PPMA: polypropylmethacrylate, OTP: orthoterphenyl, PDE: phenolphthalein-dimethyl-ether BMPS: (1,1'-bis(*p*-methoxyphenyl)cyclohexane, BMMPC: 1,1'-di(4-methoxy-5-methylphenyl)cyclohexane, BMP-BOB: (1-butyl-1-methylpyrrolidinium bis[oxalate]borate). Typically for most systems, the dynamics data points shown in the figures cover pressure ranges from $P = 1$ atm (0.1 MPa) to roughly around 200 MPa, and in some cases up to 400 or 500 MPa. Temperature values varied with system and are available in the experimental references. PVAc has been used as an example system to test different parameterization routes and data availability scenarios, so there are several slightly different parameters sets. The set listed in this table ($b \approx 3.9$), is from fitting to a very large P-dependent dynamics data set including pressures all the way up to 400 MPa. The fits of b discussed in the examples at fig. 5 were centered around somewhat lower pressures (*e.g.*, 0 to 200 MPa) and so b was closer to ≈ 3.6 to 3.7. All these values are effectively close, and in general we observe that anywhere in this range of b gives a very good data collapse in plots of $\ln\tau$ *vs.* $V_{\rm hc}/(V_{\rm free}T^b)$. Only ambient pressure dynamics data were available for P4ClS, so it was characterized using this data combined with information on $T_{\rm g}(P)$ from PVT data. See ref. [1].

			CFV Parameters			LCL EOS Characterization				References	
System	$T_{\rm g}$ (K)	γ	b	T^* (K)	$\log\tau_{\rm ref}$ (s)	$V_{\rm hc}$ (mL/g)	$r/M_{\rm w}$ (mol/g)	v (mL/mol)	$-\varepsilon$ (J/mol)	$\tau(T,P)$ data	PVT data
PVAc	305	2.6	3.90	421	−10.2	0.7583	0.1379	5.499	1805	[37,33]	[36]
PVME	242	2.5	5.89	272	−8.28	0.8665	0.1306	6.635	1782	[38]	[39]
PMPS	246	5.6	2.70	356	−16.4	0.8138	0.1147	7.095	1901	[40]	[41]
PMTS	261	5.0	2.22	465	−16.5	0.7177	0.1078	6.658	1717	[42]	[41]
PPMA	323	1.75	6.40	351	−6.25	0.8505	0.09904	8.587	1988	[43]	[36]
P4ClS	391	3.0	2.93	634	−12.3	0.7401	0.09678	7.647	2187	[44]	[36]
BMPC	241	7.0	1.77	536	−17.7	0.8179	0.2242	3.648	1677	[45]	[46]
BMMPC	261	8.5	1.61	568	−15.4	0.8338	0.1961	4.252	1858	[47]	[46]
PDE	295	4.75	2.15	548	−14.9	0.6587	0.1293	5.095	1906	[48]	[49]
OTP	244	4.35	2.71	380	−14.7	0.8202	0.1410	5.817	1720	[35]	[50]
BMPBOB	231	3.7	3.70	266	−10.6	0.7105	0.1655	4.293	1807	[51]	[34]

5 Summary

In this paper we have compared the cooperative free volume (CFV) rate model and the density scaling approach. Both models describe pressure-dependent segmental dynamics, $\tau(T,V)$, and connect a system's dynamics with its underlying thermodynamic properties. At the same time, they offer different perspectives for interpreting the behavior at the molecular level.

In density scaling, dynamics depend on the combined variable, TV^γ, where γ is the model's key parameter. This framework reflects how short-range intermolecular repulsions can dictate the dynamics by taking the behaviour of a simple repulsive (IPL) fluid as the underlying physical model, a system with key dynamic and thermodynamic properties that only depend on TV^γ.

In CFV, the dynamics of local segmental relaxation proceeds via a thermally activated, density-dependent, cooperative rate mechanism. The CFV model predicts the general form of $\log\tau \sim (1/V_{\rm free}) \times \Delta a(T)/T$. In this approach the repulsions that are "thermally accessible" contribute to the activation energy, and they must be overcome by thermal activation. Because repulsive interactions are steep, those at smaller separations are considered "thermally inaccessible" and contribute to the limiting close-packed volume, $V_{\rm hc}$. The temperature- and pressure-independent hard-core volume is used to define $V_{\rm free} = V - V_{\rm hc}$. The segmental relaxation process thus requires a degree of cooperativity ($\propto 1/V_{\rm free}$), which ultimately controls the volume dependence of the overall activation energy.

From the density scaling and the IPL fluid perspective, temperature and volume can be viewed as a single (combined) control parameter. In CFV, T and V are viewed as separate, in the sense that T controls the domain of thermal activation, and V determines spatial/structural limitations that then affect the mechanism.

A key result of this work is the analytical relationship that relates the models and connects the γ parameter to the CFV b parameter: $\gamma \approx 1/[b(V_{\rm free}/V)_{@T_{\rm g}}]$, where

$(V_{\rm free}/V)_{@T_{\rm g}}$ is the fractional free volume predicted at the ambient $T_{\rm g}$. γ and b are key to each model because they describe the relative sensitivity of a system's dynamics to changes in T *vs.* changes in V. This formula proves accurate over all the systems we have characterized. The fact that CFV and density scaling both work well is the reason why such a clear connection can be made.

Having connected the two models, we have also compared and discussed their relative predictive power: In order to characterize experimental systems, the CFV equation, $\ln\tau = (V_{\rm hc}/V_{\rm free})(T^*/T)^b + \ln\tau_{\rm ref}$, fits only three parameters to the dynamics data, while the density scaling equation, $\ln\tau = [A/(TV^\gamma)]^\phi + \ln\tau_0$, must fit four. In density scaling, neither the form of the T-dependence, or the V-dependence, is known before characterizing the data (unknown ϕ and γ). For CFV, the T-dependence is also not known beforehand (unknown b), however, the form of the V-dependence is known, because all systems follow $1/V_{\rm free}$, and importantly, $V_{\rm hc}$ and the $V_{\rm free}$ values are determined via the LCL EOS beforehand, from the thermodynamics, without the need for dynamics data. This leads to a CFV model advantage, as it remains applicable in scenarios that push the boundaries of the low data limit. In cases where there are not enough experimental data available to characterize the density scaling model, the CFV model can still be applied, and furthermore, this means it can also predict the γ parameter when it would have otherwise been unobtainable.

In this paper we have quantitatively connected the widely used density scaling approach for analyzing experimental segmental dynamics with our Cooperative Free Volume (CFV) model approach. While both routes provide physical insight to the relaxation process, the CFV model leverages analysis of thermodynamic data, which means that a minimal amount of experimental dynamics data are needed in order to achieve not only full characterization, but also significant predictive power.

We gratefully acknowledge the financial support provided by the National Science Foundation (DMR-1708542).

Author contribution statement

All authors have contributed to the preparation of this manuscript.

Appendix A. Details on applying LCL equation of state

In the following we describe the locally correlated lattice (LCL) theory equation of state (EOS) which we use to analyze pressure-volume-temperature data and then predict a system's $V_{\rm free}$ values. The LCL EOS for a compressible one-component system is given by

$$\begin{aligned}\frac{P}{k_{\rm B}T} = &\left(\frac{1}{v}\right)\ln\left[\frac{V}{V-N_{\rm m}rv}\right]\\ &+\left(\frac{3}{v}\right)\ln\left[\frac{V-(N_{\rm m}v/3)(r-1)}{V}\right]\\ &-\left(\frac{3}{v}\right)\left(\frac{(2r+1)^2}{(V/N_{\rm m}v)-(1/3)(r-1)}\right)\\ &\times\left(\frac{\exp[-\varepsilon/k_{\rm B}T]-1}{(1/3)(2r+1)\exp[-\varepsilon/k_{\rm B}T]+(V/N_{\rm m}v)-r}\right);\end{aligned} \tag{A.1}$$

$N_{\rm m}$ is the number of molecules and $k_{\rm B}$ is the Boltzmann constant. The molecular parameters are r, the number of segments (occupied lattice sites) per molecule, v, the volume per lattice site, and ε, the segment-segment nonbonded interaction energy. We determine the LCL characterization parameters (r, v, ε) by fitting the EOS to PVT data and from this we can thus calculate $V_{\rm free} = V - V_{\rm hc} = V - N_{\rm m}rv$. The product of the molecular parameters, rv, describes the volume occupied per molecule at close packing, so $V_{\rm hc} = N_{\rm m}rv$. In practice, it is convenient to report $V_{\rm hc}$ per gram, and the free volume values as either relative free volume, $V_{\rm free}/V_{\rm hc}$, or fractional free volume, $V_{\rm free}/V$. Note when we evaluate $V_{\rm free}$ at any chosen T, P point, we use the $V(T,P)$ value from the LCL EOS, *i.e.* solving eq. (A.1) at that T, P. Using the actual experimental V value (if available) would give essentially the same $V_{\rm free}$ value whenever the chosen T, P point is inside the PVT data fitting range (because the theoretical and experimental V's are very close). When extending outside the fitting range, however, is where we have found it better to stay consistently within the theory, *i.e.* using the theoretical V together with the theoretical $V_{\rm hc} = N_{\rm m}rv$, as any errors will compensate/cancel.

We try to fit the EOS over a range of PVT data that is close to the desired range of application to dynamics. Of course, how well the data ranges can be matched, will depend on data availability. The LCL parameters do shift to a degree with the fitting range, but our testing shows it will not strongly affect the analysis in most practical scenarios; it is important just to be consistent and work with a single parameterization set and its corresponding predicted properties throughout. For completeness we give the average temperature, $\langle T_{\rm fit}\rangle$, describing the fitting range of the PVT data for each of the systems listed in table 1; the values did not appear there to avoid crowding. $\langle T_{\rm fit}\rangle$ = 369, 341, 338, 338, 378, 433, 328, 328, 346, 325, 326 K respectively for PVAc, PVME, PMPS, PMTS, PPMA, P4ClS, BMPC, BMMPC, PDE, OTP, BMB-BOB.

We note that the LCL model parameters do correspond to very typical molecular level quantities. For example, a typical value for the segmental volume, v, is 8 mL/mol, which matches well with the molecular scale, corresponding to 13.3 cubic Angstroms and a segmental length of 2.37 Angstroms. rv, the hard-core molecular volume, a quantity relied on throughout this paper,

is always on the order of, but somewhat less than, the experimental total volume per molecule in a liquid, as expected. The nonbonded energetic parameter, ε, is on the order of a typical nonbonded intermolecular interaction energy. Table 1 shows ε values that range around -1700 to $-2200\,\mathrm{J/mol}$, which are on the same scale as typical Lennard-Jones parameters, *e.g.* $\varepsilon_{\mathrm{LJ}} = 996\,\mathrm{J/mol}$ for argon, $1230\,\mathrm{J/mol}$ for methane, etc. It can further be verified for small molecules that the cohesive energy per molecule at close packing, $(1/2)(4r+2)\varepsilon$, will be close to the corresponding experimental heat of vaporization. Furthermore, PVT-fitted parameters are transferable for predicting mixture properties, and in the case of small molecules, for predicting liquid-vapor equilibria (see examples in ref. [28]).

References

1. R.P. White, J.E.G. Lipson, Macromolecules **51**, 7924 (2018).
2. R.P. White, J.E.G. Lipson, J. Chem. Phys. **147**, 184503 (2017).
3. R.P. White, J.E.G. Lipson, Macromolecules **51**, 4896 (2018).
4. C. Roland, S. Hensel-Bielowka, M. Paluch, R. Casalini, Rep. Prog. Phys. **68**, 1405 (2005).
5. G. Floudas, M. Paluch, A. Grzybowski, K. Ngai, *Molecular Dynamics of Glass-Forming Systems - Effects of Pressure* (Springer, Berlin, 2011).
6. A. Grzybowski, M. Paluch, in *The Scaling of Relaxation Processes*, edited by F. Kremer, A. Loidl (Springer International Publishing, Cham, 2018) pp. 77–119.
7. L. Bohling, T.S. Ingebrigtsen, A. Grzybowski, M. Paluch, J.C. Dyre, T.B. Schroder, New J. Phys. **14**, 113035 (2012).
8. J.C. Dyre, J. Phys. Chem. B **118**, 10007 (2014).
9. N. Gnan, T.B. Schroder, U.R. Pedersen, N.P. Bailey, J.C. Dyre, J. Chem. Phys. **131**, 234504 (2009).
10. D. Fragiadakis, C.M. Roland, J. Chem. Phys. **134**, 044504 (2011).
11. R. Casalini, U. Mohanty, C.M. Roland, J. Chem. Phys. **125**, 014505 (2006).
12. R. Casalini, C.M. Roland, J. Non-Cryst. Solids **353**, 3936 (2007).
13. A.K. Doolittle, J. Appl. Phys. **22**, 1471 (1951).
14. M.L. Williams, R.F. Landel, J.D. Ferry, J. Am. Chem. Soc. **77**, 3701 (1955).
15. J.D. Ferry, *Viscoelastic Properties of Polymers*, second edition (Wiley, New York, 1970).
16. M.H. Cohen, D. Turnbull, J. Chem. Phys. **31**, 1164 (1959).
17. R.P. White, J.E.G. Lipson, Macromolecules **49**, 3987 (2016).
18. R.P. White, J.E.G. Lipson, ACS Macro Lett. **6**, 529 (2017).
19. A. Debot, R.P. White, J.E.G. Lipson, S. Napolitano, ACS Macro Lett. **8**, 41 (2019).
20. W. Hoover, M. Ross, Contemp. Phys. **12**, 339 (1971).
21. Y. Hiwatari, H. Matsuda, T. Ogawa, N. Ogita, A. Ueda, Prog. Theor. Phys. **52**, 1105 (1974).
22. U.R. Pedersen, N.P. Bailey, T.B. Schroder, J.C. Dyre, Phys. Rev. Lett. **100**, 015701 (2008).
23. U.R. Pedersen, T.B. Schroder, J.C. Dyre, Phys. Rev. Lett. **105**, 157801 (2010).
24. D. Coslovich, C.M. Roland, J. Chem. Phys. **131**, 151103 (2009).
25. D. Coslovich, C.M. Roland, J. Phys. Chem. B **112**, 1329 (2008).
26. D. Coslovich, C.M. Roland, J. Chem. Phys. **130**, 014508 (2009).
27. I. Avramov, J. Non-Cryst. Solids **262**, 258 (2000).
28. J.E.G. Lipson, R.P. White, J. Chem. Eng. Data **59**, 3289 (2014).
29. G. Adam, J.H. Gibbs, J. Chem. Phys. **43**, 139 (1965).
30. R. Casalini, C.M. Roland, Phys. Rev. Lett. **113**, 085701 (2014).
31. K. Koperwas, A. Grzybowski, S.N. Tripathy, E. Masiewicz, M. Paluch, Sci. Rep. **5**, 17782 (2015).
32. M. Goldstein, J. Phys. Chem. **77**, 667 (1973).
33. C. Roland, R. Casalini, Macromolecules **36**, 1361 (2003).
34. M. Paluch, S. Haracz, A. Grzybowski, M. Mierzwa, J. Pionteck, A. Rivera-Calzada, C. Leon, J. Phys. Chem. Lett. **1**, 987 (2010).
35. M. Naoki, H. Endou, K. Matsumoto, J. Phys. Chem. **91**, 4169 (1987).
36. P. Zoller, D. Walsh, *Standard Pressure-Volume-Temperature Data for Polymers* (Technomic Pub Co., Lancaster, PA, 1995).
37. W. Heinrich, B. Stoll, Colloid Polym. Sci. **263**, 873 (1985).
38. R. Casalini, C. Roland, J. Chem. Phys. **119**, 4052 (2003).
39. T. Ougizawa, G.T. Dee, D.J. Walsh, Macromolecules **24**, 3834 (1991).
40. M. Paluch, C. Roland, S. Pawlus, J. Chem. Phys. **116**, 10932 (2002).
41. M. Paluch, R. Casalini, A. Patkowski, T. Pakula, C. Roland, Phys. Rev. E **68**, 031802 (2003).
42. M. Paluch, S. Pawlus, C. Roland, Macromolecules **35**, 7338 (2002).
43. P. Panagos, G. Floudas, J. Non-Cryst. Solids **407**, 184 (2015).
44. A. Panagopoulou, S. Napolitano, Phys. Rev. Lett. **119**, 097801 (2017).
45. S. Hensel-Bielowka, J. Ziolo, M. Paluch, C. Roland, J. Chem. Phys. **117**, 2317 (2002).
46. M. Paluch, C. Roland, R. Casalini, G. Meier, A. Patkowski, J. Chem. Phys. **118**, 4578 (2003).
47. R. Casalini, M. Paluch, C. Roland, Phys. Rev. E **67**, 031505 (2003).
48. R. Casalini, M. Paluch, C.M. Roland, J. Phys.: Condens. Matter **15**, S859 (2003).
49. M. Paluch, R. Casalini, A. Best, A. Patkowski, J. Chem. Phys. **117**, 7624 (2002).
50. M. Naoki, S. Koeda, J. Phys. Chem. **93**, 948 (1989).
51. A. Rivera-Calzada, K. Kaminski, C. Leon, M. Much, J. Phys. Chem. B **112**, 3110 (2008).